

Optical quenching of metastable magnesium

Nils Rehbein, Tanja E. Mehlstäubler, Jochen Keupp, Karsten Moldenhauer, Ernst M. Rasel,* and Wolfgang Ertmer
Institut für Quantenoptik, Leibniz Universität Hannover, Welfengarten 1, 30167 Hannover, Germany

Albane Douillet

Laboratoire Kastler Brossel, Université Pierre et Marie Curie, Case 74, 4 Place Jussieu, 75252 Paris, France
and Département de Physique et Modélisation, Université d'Evry Val d'Essonne, Boulevard F. Mitterrand, 91025 Evry cedex, France

Volker Michels

Deutsches Elektronen Synchrotron, Notkestrasse 85, 22607 Hamburg, Germany

Sergey G. Porsev

Petersburg Nuclear Physics Institute, Gatchina, Leningrad district, 188300 Russia

Andrei Derevianko

Physics Department, University of Nevada, Reno, Nevada 89557, USA

Charlotte Froese Fischer and Georgio I. Tachiev

Department of Computer Science, Vanderbilt University, Box 1679B, Nashville, Tennessee 37235, USA

Vitaly G. Pal'chikov

Institute for Time and Space at National Research Institute for Physical-Technical and Radiotechnical Measurements, Mendeleevo, Moscow Region, 141579 Russia

(Received 24 September 2006; revised manuscript received 22 June 2007; published 8 October 2007)

Doppler cooling on narrow transitions has become a crucial technique for preparing ultracold samples of alkaline-earth-metal and alkaline-earth-metal-like atoms. For lighter species, such as calcium and magnesium, this technique relies on artificial broadening (*quenching*) of the upper level of the narrow line. We report on quenching experiments on a ^{24}Mg atomic beam. The branching ratio of the $(3s4s)^1S_0$ state was determined to be $\beta=(1.33\pm 0.53)\times 10^{-5}$ from the measured quenching efficiency. The branching ratio combined with the known linewidth of this state yields a transition rate for $(3s3p)^3P_1\rightarrow(3s4s)^1S_0$ of $\Gamma_{23}=283\pm 114\text{ s}^{-1}$, i.e., one order of magnitude smaller than estimated from semiempirical data. We have applied different numerical approaches, including *ab initio* relativistic many-body calculations, to compute the transition probabilities of the $(3s3p)^3P_1\rightarrow(3s4s)^1S_0$ and $(3s3p)^1P_1\rightarrow(3s4s)^1S_0$ transitions. The results are in good agreement with our experimental observation. With the measured branching ratio, we expect a transfer efficiency of Doppler-cooled atoms into a quench magneto-optical trap (QuenchMOT) of approximately 1% for our experimental parameters. According to our simulations, the transfer efficiency can be increased by one order of magnitude for lower ensemble temperatures as recently demonstrated by two-photon cooling in our uv MOT.

DOI: [10.1103/PhysRevA.76.043406](https://doi.org/10.1103/PhysRevA.76.043406)

PACS number(s): 32.80.Pj, 32.70.Cs, 31.15.Ar, 31.15.Gy

I. INTRODUCTION

The alkaline-earth-metal and alkaline-earth-metal-like atoms have attracted intensive research interest due to their unique spectroscopic properties [1–9]. Their intercombination transitions, with natural linewidths as low as a few tens of a microhertz, are ideally suited for optical frequency standards and future optical atomic clocks. Here, the quality factor, which is defined as the ratio of the transition frequency ν and the achieved resolution $\delta\nu$ ($Q=\nu/\delta\nu$), can reach values of $Q\approx 10^{18}$. The simple electronic structure of the alkaline-earth metals, on the other hand, is well suited for theoretical modeling. Hence, they are ideal test systems for systematic studies of, e.g., cold collisions [10–13]. To fully exploit this

potential, however, the reliable preparation, i.e., trapping and cooling, of large identical samples of ultracold ensembles is essential. One of the most promising techniques for frequency metrology in the optical domain is the concept of the “lattice clock.” Based on laser-cooled strontium atoms, this was first demonstrated by Katori and co-workers [4]. This approach combines the high stability achievable with neutral atoms due to the large number of quantum absorbers with the high accuracy seen in trapped ions due to their strong confinement [14–16]. Efficiently loading and storing cold atoms into an optical dipole trap or lattice requires a sufficiently low atomic temperature, typically tens of a microkelvin. Unlike in many other atomic species, e.g., rubidium, where trapping, cooling, and even creating a Bose-Einstein condensate has become a routine task, the preparation of large atomic ensembles in this temperature regime remains a challenge for alkaline-earth metals. In particular, the absence of magnetic sublevels in the ground state of their bosonic iso-

*rasel@iqo.uni-hannover.de

topes inhibits standard sub-Doppler cooling mechanisms. The possibility of reaching the recoil temperature limit in the alkaline-earth metals ($10 \mu\text{K}$ in the case of magnesium) by exploiting the high velocity selectivity of their narrow inter-combination transitions has already been pointed out in 1989 [17]. In strontium, this has been realized in a sophisticated two-stage cooling scheme [18,19].

In calcium and magnesium, however, the natural lifetimes of the metastable states are too long for efficient cooling. We therefore proposed to artificially reduce the lifetime of the metastable level by *quenching* with an additional laser coupling to a fast decay channel back to the ground state. The resulting enhancement of the scattering rate is governed by the quenching laser power and the branching ratio between the quenching transition and the fast decay channel [20].

In calcium, quench cooling was demonstrated in 2001 [20,21], thus confirming our theoretical model. From the experimentally observed quenching rates, a branching ratio of the order of 10^{-4} could be inferred [20]. For the initial modeling of this cooling scheme in magnesium [22], we used a branching ratio of $\beta_{\text{Mg}} \approx 1.3 \times 10^{-4}$, which was estimated from semiempirical data given by Kurucz [23]. Recent theoretical work, as well as experience from experiments with calcium, however, suggests a significantly lower branching ratio. To resolve this discrepancy, we performed spectroscopy of the $(3s3p)^3P_1 \rightarrow (3s4s)^1S_0$ transition on a magnesium atomic beam, as well as numerical calculations based on different methods. We discuss the impact of the lower branching ratio as well as the effect of a reduced initial atomic temperature, which can, e.g., be achieved by two-photon cooling [24–26], on the efficiency of quench cooling.

This paper is structured as follow. In Sec. II, we present our quenching experiments on a magnesium atomic beam. From the observations, we determine the branching ratio of the $(3s4s)^1S_0$ level and the decay rate of the $(3s3p)^3P_1 \rightarrow (3s4s)^1S_0$ quenching transition. In Sec. III, we present and discuss the different computational approaches used to calculate the decay rate of the quenching transition. In our conclusions in Sec. IV, we confront our experimental observations with the theoretical predictions. We use our results for the branching ratio to improve our model of quench cooling of magnesium and discuss the perspectives for the optical magnesium frequency standard.

II. QUENCHING EXPERIMENTS

A. Magnesium beam setup

We have studied quenching of the metastable $(3s3p)^3P_1$ level using a beam apparatus designed for Ramsey-Bordé interferometry [27–29]. Here, we use the setup in a modified form as shown in Fig. 1. A collimated beam of magnesium atoms subsequently interacts with linearly ($\vec{E} \parallel \vec{e}_z$) polarized laser light of 457 and 462 nm. This configuration is obtained by placing two retroreflecting mirrors into the original Ramsey-Bordé interferometer beam path (457 nm laser only) and results in parallel beams for the 457 and 462 nm lasers. The interaction region is shielded against external magnetic fields, and a homogeneous magnetic field in the z direction

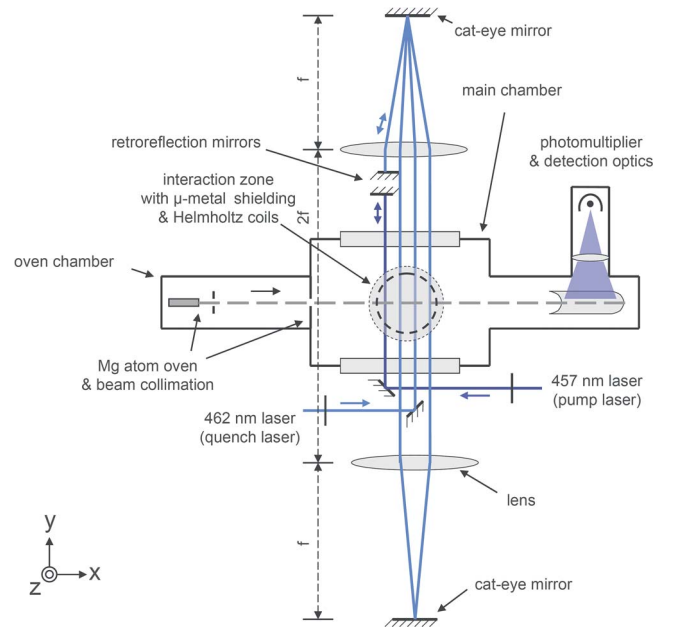


FIG. 1. (Color online) Modified Ramsey-Bordé setup used for quenching experiments.

can be applied to define the quantization axis. When driving the $(3s^2)^1S_0 \rightarrow (3s3p)^3P_1$ transition with the 457 nm laser, fluorescence from the decay of the metastable level $(3s3p)^3P_1$ back to the ground state $(3s^2)^1S_0$ is observed by a photomultiplier tube (PMT). The count rate N_0 is directly proportional to the population of the metastable level. Additionally driving the $(3s3p)^3P_1 \rightarrow (3s4s)^1S_0$ transition with the 462 nm (quenching) laser leads to a depletion of the metastable level, which is observed as a drop of the count rate. Figure 2 shows the relevant transitions. We have measured the frequency of the quenching transition as

$$\nu_{23} = 648\,537.76 \pm 0.04 \text{ GHz.}$$

Taking into account the uncertainty of the measurement, this agrees very well with earlier observations [30].

B. Determination of branching ratio and decay rate

The general formalism for quenching the metastable level has already been communicated in earlier publications

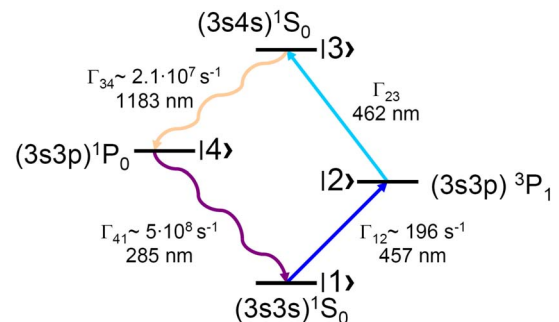


FIG. 2. (Color online) Relevant transitions for quenching in ^{24}Mg .

[22,31]. As derived in [31], the ratio of the population in the metastable state with and without quenching is given by

$$S = \exp\left(-\frac{\Omega_{23}^2}{\Gamma_{34}} \tau\right), \quad (1)$$

where τ is the duration of the interaction with the quenching laser. Using the expression for the Rabi frequency of the quenching laser,

$$\Omega_{23} = C_{CG} \sqrt{\frac{3\lambda_{23}^3 I_{23} \Gamma_{23}}{2\pi\hbar c}} \quad (2)$$

we obtain for an infinitely small interaction region dx and an atom velocity v_x ,

$$S(dx, v_x) = \exp\left(-\frac{\lambda_{23}^3 I_{23} \beta dx}{2\pi\hbar c v_x}\right), \quad (3)$$

where we have introduced the branching ratio $\beta := \Gamma_{23}/\Gamma_{34}$ and the Clebsch-Gordan coefficient of the quenching transition $C_{CG} = 1/\sqrt{3}$. λ_{23} and I_{23} are the quenching laser wavelength and intensity, respectively, and Γ_{23} is the quenching transition linewidth (cf. Fig. 2). The observed fluorescence signal without quenching can be calculated using the standard Rabi formalism. The excitation probability to the metastable level $(3s3p)^3P_1$ is

$$p_2(dx, v) = \sin^2\left(\frac{\Omega_{12} dx}{2v_x}\right). \quad (4)$$

Since the fluorescence signal is observed at a distance $d = 46$ cm downstream the atomic beam within a detection zone of length $l = 10$ cm, it is reduced by a velocity-dependent factor,

$$\eta(v_x) = \exp\left(-\frac{\Gamma_{12} d}{v_x}\right) \left[1 - \exp\left(-\frac{\Gamma_{12} l}{v_x}\right)\right], \quad (5)$$

and depends on the longitudinal velocity distribution for the atomic beam [32],

$$f(v_x) = \frac{v_x^3}{2\tilde{v}^4} \exp\left(-\frac{v_x^2}{2\tilde{v}^2}\right) \quad \text{where } \tilde{v} = \sqrt{\frac{k_B T}{M}}. \quad (6)$$

Here, M denotes the atomic mass, T is the oven temperature, and k_B is Boltzmann's constant.

The observed signal ratio N/N_0 (where N is the reduced PMT count rate with the quenching laser on) is obtained by integration over all longitudinal velocities v_x and the (transverse) intensity profiles of the laser beams.

Thus, for an atomic beam radius r , the expected signal decrease is

$$\frac{N}{N_0} = \frac{\int_0^r \int_0^\infty f(v_x) p_2(v_x, z) S(v_x, z, \beta) \eta(v_x) dv_x dz}{\int_0^r \int_0^\infty f(v_x) p_2(v_x, z) \eta(v_x) dv_x dz}. \quad (7)$$

This equation is evaluated numerically.

A small ($B_z \approx 1.0$ G) magnetic field was applied in the z direction to define the quantization axis and compensate for

TABLE I. Typical experimental parameters and uncertainties.

Parameter	Symbol	Value
Pump laser power	P_{12}	73 ± 3.7 mW
Quench laser power	P_{23}	286 ± 14 mW
Pump laser radius (x)	w_{0x12}	1.09 ± 0.05 mm
Pump laser radius (z)	w_{0z12}	1.11 ± 0.06 mm
Quench laser radius (x)	w_{0x23}	0.63 ± 0.03 mm
Quench laser radius (z)	w_{0z23}	0.73 ± 0.04 mm
Atomic beam radius	r	0.8 ± 0.2 mm
Oven temperature	T	678 ± 34 K
Typical signal decrease	N/N_0	0.791 ± 0.024

any residual fields. To determine the branching ratio, we averaged the results of a series of 15 measurements in total. In the experiments, the total excitation and quenching laser powers were varied between 73 and 88 mW and 122 and 298 mW, respectively. Table I summarizes typical experimental parameters.

From the experimental results, we obtain

$$\beta^{\text{obs}} = (1.33 \pm 0.53) \times 10^{-5}$$

and

$$\Gamma_{23}^{\text{obs}} = 283 \pm 114 \text{ s}^{-1}.$$

For Γ_{34} , we have used the value given by Jönsson, i.e., $\Gamma_{34} = (2.13 \pm 0.01) \times 10^7 \text{ s}^{-1}$ [33], and the error estimation is based on the uncertainties of the experimental parameters given in Table I. The error in β^{obs} and Γ_{23}^{obs} , respectively, is governed by the uncertainties in measuring the fluorescence signal decrease N/N_0 and the (quenching) laser power P_{23} , and by the uncertainty in the radius of the atomic beam.

III. THEORY

The transition probabilities of the relevant transitions $(3s3p)^3P_1 \rightarrow (3s4s)^1S_0$ and $(3s3p)^1P_1 \rightarrow (3s4s)^1S_0$ have also been determined by three different theoretical approaches for comparison. The results derived from a semiempirical model and two different *ab initio* models are presented and compared.

The first *ab initio* approach combines the configuration interaction method with many-body perturbation theory (CI+MBPT) [34,35]. Many-body perturbation theory is able to precisely determine the correlations of the core electrons, whereas CI describes correlations between valence electrons accurately. By MBPT an effective CI Hamiltonian is constructed which includes additional terms to account for core-core and core-valence correlations. Energy levels and wave functions are then calculated following the well-known CI method.

The second *ab initio* approach, multiconfiguration Hartree-Fock (MCHF), approximates the wave function by a linear combination of the configuration state functions (CSFs), basis functions of the configuration model [36]. Un-

TABLE II. The *ab initio*-calculated reduced electric-dipole matrix elements (a.u.) and transition probabilities A (s^{-1}) for the $(3s3p)^3P_1 \rightarrow (3s4s)^1S_0$ and $(3s3p)^1P_1 \rightarrow (3s4s)^1S_0$ transitions for Mg I.

	CI	CI+MBPT	MCHF+BP	CI	CI+MBPT	MCHF+BP
Matrix element		$\langle 3s3p^3P_1 D 3s4s^1S_0 \rangle$			$\langle 3s3p^1P_1 D 3s4s^1S_0 \rangle$	
L gauge	0.00297	0.00323	0.00324	4.34	4.25	4.26
V gauge	0.00318	0.00331	0.00337	4.30	4.22	4.31
Final value	0.00323(13)		0.00324	4.25(4)		4.26
A	214(17)		215	$2.21(4) \times 10^7$		2.22×10^7

like the ordinary Hartree-Fock method, MCHF accounts for correlations in the motion of the electrons. As long as the number of valence electrons is not too large, these correlations are well described by this method. Relativistic effects are included via the Breit-Pauli Hamiltonian.

Additionally, a semiempirical approach was used, which, as opposed to precise many-body *ab initio* methods, does not require large computer resources and is straightforward to apply.

A. Many-body *ab initio* calculations

In the CI+MBPT approach, the energies and wave functions are determined from the Schrödinger equation

$$H_{\text{eff}}(E_n)\Phi_n = E_n\Phi_n, \quad (8)$$

where the effective Hamiltonian is defined as

$$H_{\text{eff}}(E) = H_{\text{FC}} + \Sigma(E). \quad (9)$$

Here H_{FC} is the Hamiltonian in the frozen core approximation and Σ is the energy-dependent correction, involving core excitations. The operator Σ completely accounts for the second order of perturbation theory. The higher orders of MBPT can be included indirectly. For this goal one can introduce an energy shift δ and replace $\Sigma(E) \rightarrow \Sigma(E - \delta)$ in the effective Hamiltonian H_{eff} . We have determined δ from a fit of theoretical energy levels to the experimental spectrum. Such an optimized effective Hamiltonian was used for calculations of the wave functions and low-lying energy levels.

Atomic observables were calculated with effective operators [35]. To obtain an effective electric-dipole operator, we solved the random-phase approximation (RPA) equations, thus summing a certain sequence of many-body diagrams to all orders of MBPT. Excitations from all core shells were included in the RPA setup. To check the consistency of the calculations, we employed both length (L) and velocity (V) gauges for the electric-dipole operator. The computational procedure is described in [37,38].

We considered Mg as an atom with two valence electrons above the closed core $[1s, \dots, 2p^6]$. The one-electron basis set for Mg included $1s$ – $13s$, $2p$ – $13p$, $3d$ – $12d$, and $4f$ – $11f$ orbitals, where the core and $3s$, $4s$, $3p$, $4p$, $3d$, $4d$, and $4f$ orbitals were Dirac-Hartree-Fock (DHF) ones, while all the rest were virtual orbitals. The orbitals $1s$ – $3s$ were constructed by solving the DHF equations in the V^N approximation, the $3p$ orbitals were obtained in the V^{N-1} approximation, and $4s$, $4p$, $3d$, $4d$, and $4f$ orbitals were constructed in

the V^{N-2} approximation. We determined virtual orbitals using a recursive procedure employed in previous works [37,38]. Solving the eigenvalue problem, we obtained wave functions, constructed effective dipole operators, and determined the transition amplitudes. The comparison of the CI and the CI+MBPT values allows us to estimate the accuracy of our calculations. In general, dipole amplitudes calculated in the velocity gauge are more sensitive to many-body corrections; we employ the length form of the dipole operator in our final tabulation. Table II reveals that the many-body effects change the singlet-triplet L -gauge amplitude by 8% and the singlet-singlet L -gauge amplitude by 2%. Further, the MBPT corrections bring the length- and velocity-form results into a closer agreement. We consider the impossibility of accounting for all the orders of many-body perturbation theory as a major source of uncertainty of the CI+MBPT method. In addition, we take into account the proximity of the amplitudes obtained in the L and V gauges. We conservatively estimate the uncertainties for the $(3s3p)^{1,3}P_1 \rightarrow (3s4s)^1S_0$ transition amplitudes as 50% of the many-body corrections in the length gauge. The uncertainties determined in this way are 1% for the singlet-singlet transition and 4% for the singlet-triplet transition. The final values for the $(3s3p)^{1,3}P_1 \rightarrow (3s4s)^1S_0$ transition amplitudes, are given in Table II.

For comparison, we used as a second approach the CI+MCHF method [36] to calculate the quench transition amplitude. The MCHF method was applied to determine the orbital basis for the Breit-Pauli wave functions which were simultaneously optimized for the relevant nonrelativistic terms. Due to this procedure, the calculations for electric dipole transitions using the J -dependent wave functions are performed with orbitals that are nonorthogonal between initial and final states. For this, the biorthogonal transformation method was used [39].

For each term included in the Breit-Pauli (BP) configuration interaction calculation, the wave function is expanded in a linear combination of configuration state functions. In generating these expansions, both the valence correlation and core-valence correlation were included. The valence correlation includes all configuration state functions of the form $2s^2 2p^6 n l n' l'$. The effect of core-valence correlation (polarization of the core) was represented by configuration state functions in which one of the core orbitals, either $2s$ or $2p$ ($1s$ was assumed to be inactive) was excited along with one outer orbital. For this purpose, a multireference set consisting of all configuration states of the form $2s^2 2p^6 3 l n' l'$ was established, with $n'=3$ or 4 and $l' \leq 3$. Thus the occupied

outer orbitals are $3s$, $3p$, $3d$, $4s$, $4p$, $4d$, and $4f$ and the virtual correlation orbitals were taken to be $5s$, $5p$, $5d$, $5f$, $5g$, ..., $9s$, $9p$, $9d$, $9f$, $9g$, $9h$, and $9i$. Core-valence excitations were applied to each member of the multireference set. Core and outer orbitals could be excited to either an outer orbital or a virtual correlation orbital.

In order to monitor convergence, it is convenient to perform a series of calculations of increasing size. For example, a calculation is considered an $n=4, 5, 6, \dots, 9$ calculation if the maximum principal quantum number of an orbital used in generating configuration states is restricted to 4, 5, 6, ..., 9, respectively. For an exact wave function, the length and velocity forms should agree exactly. In our case convergence has been reached within our model calculation, but the two values differ by 1%. Correlation in the core, which affects transitions differently, has been omitted in our approach: for example, for the $(3s3p)^3P \rightarrow (3s3d)^3D$ transitions, the two forms of the line strength agree to 0.5%. The calculated reduced matrix elements for the $(3s3p)^{1,3}P_1 \rightarrow (3s4s)^1S_0$ transitions are given in Table II.

B. Semiempirical calculations

Semiempirical approaches based on a model potential (MP) method yielded quite accurate results, in particular for atoms with a single valence electron or the one-electron excited states of an atom with a few valence electrons [40]. In the present paper, we have introduced exact long-range polarization terms [41], in order to study atomic systems by conventional CI methods. The corresponding two-electron operator in the Schrödinger equation includes both the Coulomb interaction of the valence electrons and induced core effects. We expanded the two-electron eigensolutions in terms of antisymmetrized products of the eigenfunctions of the one-electron equation with the model potential. The relativistic perturbations are the spin-orbit, spin-other-orbit, and spin-spin interactions and the expansion is carried out to the first order.

The single-electron equation was solved variationally by expanding the solutions for the radial parts with basis sets constructed from 35 B splines [42]. These one-electron orbitals served as a basis to solve the two-electron equation with an effective dipole operator. The final results of the calculations for the Einstein coefficients by using the L gauge are

$$A[(3s3p)^1P_1 \rightarrow (3s4s)^1S_0] = 2.5 \times 10^7 \text{ s}^{-1}$$

and

$$A[(3s3p)^3P_1 \rightarrow (3s4s)^1S_0] = 200 \text{ s}^{-1}.$$

The accuracy of our MP calculations is limited by the accuracy of the expansion of the CI basis sets for small radial coordinates. These results are in reasonable agreement with the precise *ab initio* data presented in Table II.

IV. CONCLUSIONS AND OUTLOOK

In conclusion, we have determined the branching ratio of the $(3s4s)^1S_0$ level and the decay rate of the $(3s3p)^3P_1 \rightarrow (3s4s)^1S_0$ transition in magnesium experimentally and by

ab initio relativistic many-body calculations. Within the limits of their uncertainty, the experimental results

$$\beta^{\text{obs}} = (1.33 \pm 0.53) \times 10^{-5}$$

and

$$\Gamma_{23}^{\text{obs}} = 283 \pm 114 \text{ s}^{-1}$$

are in good agreement with the results of the most accurate *ab initio* calculation,

$$\beta^{\text{calc}} = (9.7 \pm 0.77) \times 10^{-6}$$

and

$$\Gamma_{23}^{\text{calc}} = 214 \pm 17 \text{ s}^{-1}.$$

These results are about one order of magnitude smaller than the values derived from the semiempirical data of Kurucz [23].

This has important consequences for quench cooling of magnesium. In [22], we published a theoretical model to estimate the cooling efficiency as a function of important experimental parameters. Optimizing the transfer efficiency of the precooled atoms into the quench magneto-optical trap (QuenchMOT), we showed that the branching ratio drives the requirements for the quench laser intensity and the initial ensemble temperature. For a given quench laser intensity, the quenching rate scales linearly with the branching ratio β and thus is reduced by one order of magnitude according to the new results.

The scaling behavior of the transfer efficiency with the initial atomic temperature can be modeled by considering that only atoms slower than the QuenchMOT capture velocity v_{cap} are transferred into the ultracold regime. These correspond to the fraction of atoms initially in the velocity interval $v \in [0, v_{\text{cap}}]$, i.e.,

$$\eta \approx \int_0^{v_{\text{cap}}} f(v) dv, \quad (10)$$

where $f(v)$ is the Maxwell-Boltzmann velocity distribution for an atomic temperature T_{ini} .

As long as the capture velocity of the QuenchMOT is small compared to the Gaussian width of the velocity distribution of the precooled ensemble and the saturation of the quench transition is low, the transfer efficiency scales according to [22]

$$\eta(P_q, T_{\text{ini}}) \propto (P_q/T_{\text{ini}})^{3/2}. \quad (11)$$

Scaling our first simulation results [22], we arrive at a transfer efficiency of about 1% for our measured branching ratio. This value is derived for powers of 50 and 20 mW per beam of the quenching and cooling lasers, respectively, with laser waists of 2 mm. As initial atomic temperature, we choose 4 mK rather than the usual Doppler limit of 1.9 mK. This value is usually reached within our magnesium uv MOT and is caused, e.g., by additional heating processes due to spatial inhomogeneities of the MOT laser beam profiles (cf. [43]). Equation (11) also indicates that the transfer efficiency can be increased by lowering the initial temperature. For magnesium, coherent two-photon cooling is an attractive

scheme for this purpose. In the scheme, the velocity selectivity of the standard Doppler cooling is enhanced by using a coherent two-photon process. This cooling effect was first observed in a magnesium optical molasses [31] and in a MOT [25] using the $(3s3p)^1P_1 \rightarrow (3s3d)^1D_2$ transition. Recently, we have achieved a temperature reduction by a factor of 4 within our magnesium MOT, corresponding to a final atomic temperature of 1.1 mK. A temperature reduction by up to one order of magnitude seems feasible [26]. Reducing the temperature of the precooled ensemble by a factor 4 will raise the transfer efficiency to the QuenchMOT by approximately one order of magnitude. Using this scheme for precooled, we expect to prepare up to 10^6 atoms at the recoil limit of $10 \mu\text{K}$ in a QuenchMOT.

Quench cooling, thus, remains a promising technique to efficiently load and cool atoms into dipole traps. Here, the required laser power is significantly reduced as the quench laser beams can be more tightly focused. For dipole traps, which are operated at the magic wave length, temperatures even below the microkelvin range can be expected by quench cooling atoms into the narrow velocity selective dark states as demonstrated for one dimension in [45] or by velocity selective coherent population trapping in three dimensions [44].

This opens up promising perspectives for further research toward a magnesium optical atomic clock. First, using microkelvin cold samples will improve the stability and accuracy potential of the magnesium optical frequency standard. As it was shown in [2], the potential stability of the standard at the limit of quantum projection noise,

$$\sigma_y(\tau) \approx 1/[Q(\text{SNR})\sqrt{\tau/1 \text{ s}}], \quad (12)$$

could improve from its present $\sigma_y(\tau=1 \text{ s}) \approx 8 \times 10^{-14}$ to below 10^{-15} .

Second, large microkelvin cold atomic samples facilitate efficient loading of an optical dipole trap or lattice, in order to achieve strong confinement of the spectroscopic ensemble. The trap would be operated at the “magic wavelength” where the Stark shifts for the ground and excited states of the clock transition are equal by definition. For the relevant clock transitions in magnesium, the magic wavelengths are in the blue spectral range (435–470 nm) [31,46]. In this wavelength region, experimentally feasible trap depths are in the range of $10 \mu\text{K}$, and thus ultracold atoms are needed for efficient loading. In such a trap, following, e.g., the concept demonstrated for strontium by Takamoto *et al.* [4], one could take advantage of the full potential of the ultranarrow intercombination transitions. Using the ultranarrow ($\gamma=70 \mu\text{Hz}$) $(3s^2)^1S_0 \rightarrow (3s3p)^3P_2$ transition [47], magnesium ultimately provides a spectroscopic Q factor of $Q \approx 10^{18}$.

ACKNOWLEDGMENTS

This work has been funded by the Deutsche Forschungsgemeinschaft (SFB 407, EGC 665) and the European Union (CAUAC). The work of S.P. was supported in part by the Russian Foundation for Basic Research under Grant No. 04-02-16345-a. The work of A.D. was partially supported by the National Science Foundation. The work of C.F.F. and G.T. was supported by the Chemical Sciences, Geosciences and Biosciences Division, Office of Basic Energy Sciences, Office of Science, U.S. Department of Energy. One of the authors (V.G.P.) wishes to express thanks for the hospitality of the Institute of Quantum Optics (University of Hannover).

-
- [1] C. Degenhardt, H. Stoehr, C. Lisdat, G. Wilpers, H. Schnatz, B. Lipphardt, T. Nazarova, P. E. Pottie, U. Sterr, J. Helmcke, and F. Riehle, *Phys. Rev. A* **72**, 062111 (2005).
 - [2] J. Keupp, A. Douillet, T. E. Mehlstäubler, N. Rehbein, E. M. Rasel, and W. Ertmer, *J. Phys. D* **36**, 289 (2005).
 - [3] T. Ido, Th. H. Loftus, M. M. Boyd, A. D. Ludlow, K. W. Holman, and J. Ye, *Phys. Rev. Lett.* **94**, 153001 (2005).
 - [4] M. Takamoto, F. L. Hong, R. Higashi, und H. Katori, *Nature (London)* **435**, 321 (2005).
 - [5] G. Ferrari, P. Cancio, R. Drullinger, G. Giusfredi, N. Poli, M. Prevedelli, C. Toninelli, and G. M. Tino, *Phys. Rev. Lett.* **91**, 243002 (2003).
 - [6] R. Le Targat, X. Baillard, M. Fouché, A. Bruschi, O. Tcherbakoff, G. D. Rovera, and P. Lemonde, *Phys. Rev. Lett.* **97**, 130801 (2006).
 - [7] C. W. Hoyt, Z. W. Barber, C. W. Oates, T. M. Fortier, S. A. Diddams, and L. Hollberg, *Phys. Rev. Lett.* **95**, 083003 (2005).
 - [8] L. Hollberg, C. W. Oates, G. Wilpers, C. W. Hoyt, Z. W. Barber, S. A. Diddams, W. H. Oskay, and J. C. Bergquist, *J. Phys. B* **38**, 469 (2005).
 - [9] Y. Takasu, K. Maki, K. Komori, T. Takano, K. Honda, M. Kumakura, T. Yabuzaki, and Y. Takahashi, *Phys. Rev. Lett.* **91**, 040404 (2003).
 - [10] D. Hansen and A. Hemmerich, *Phys. Rev. Lett.* **96**, 073003 (2006).
 - [11] R. Ciurylo, E. Tiesinga, S. Kotochigova, and P. S. Julienne, *Phys. Rev. A* **70**, 062710 (2004).
 - [12] A. Derevianko, S. G. Porsev, S. Kotochigova, E. Tiesinga, and P. S. Julienne, *Phys. Rev. Lett.* **90**, 063002 (2003).
 - [13] M. Machholm, P. S. Julienne, and K.-A. Suominen, *Phys. Rev. A* **65**, 023401 (2002).
 - [14] E. Peik, T. Schneider, and C. Tamm, *J. Phys. B* **39**, 145 (2006).
 - [15] H. S. Margolis, G. P. Barwood, G. Huang, H. A. Klein, S. N. Lea, K. Szymaniec, and P. Gill, *Science* **206**, 1355 (2004).
 - [16] S. Bize, S. A. Diddams, U. Tanaka, C. E. Tanner, W. H. Oskay, R. E. Drullinger, T. E. Parker, T. P. Heavner, S. R. Jefferts, L. Hollberg, W. M. Itano, and J. C. Bergquist, *Phys. Rev. Lett.* **90**, 150802 (2003).
 - [17] H. Wallis and W. Ertmer, *J. Opt. Soc. Am. B* **6**, 2211 (1989).
 - [18] H. Katori, T. Ido, Y. Isoya, and M. Kuwata-Gonokami, *Phys. Rev. Lett.* **82**, 1116 (1999).
 - [19] K. R. Vogel, T. P. Dineen, A. Gallagher, and J. L. Hall, *IEEE*

- Trans. Instrum. Meas. **48**, 618 (1999).
- [20] T. Binnewies, G. Wilpers, U. Sterr, F. Riehle, J. Helmcke, T. E. Mehlstäubler, E. M. Rasel, and W. Ertmer, Phys. Rev. Lett. **87**, 123002 (2001).
- [21] E. A. Curtis, C. W. Oates, and L. Hollberg, Phys. Rev. A **64**, 031403(R) (2001).
- [22] T. E. Mehlstäubler, J. Keupp, A. Douillet, N. Rehbein, E. M. Rasel, and W. Ertmer, J. Opt. B: Quantum Semiclassical Opt. **5**, S183 (2003).
- [23] R. L. Kurucz and B. Bell, Atomic Line Data, Kurucz CD-ROM No. 23 (Cambridge, MA, Smithsonian Astrophysical Observatory), 1995.
- [24] W. C. Magno, R. L. Cavasso Filho, and F. C. Cruz, Phys. Rev. A **67**, 043407 (2003).
- [25] N. Malossi, S. Damkjaer, P. L. Hansen, L. B. Jacobsen, L. Kindt, S. Sauge, J. W. Thomsen, F. C. Cruz, M. Allegrini, and E. Arimondo, Phys. Rev. A **72**, 051403(R) (2005).
- [26] K. Moldenhauer, J. Friebe, T. E. Mehlstäubler, N. Rehbein, M. Riedmann, E. M. Rasel, and W. Ertmer, *Book of Abstracts XXth International Conference on Atomic Physics* (Innsbruck, Austria, 2006), p. 153.
- [27] K. Sengstock, U. Sterr, J. H. Müller, V. Rieger, D. Bettermann, and W. Ertmer, Appl. Phys. B: Lasers Opt. **59**, 99 (1994).
- [28] F. Ruschewitz, J. L. Peng, H. Hinderthür, N. Schaffrath, K. Sengstock, and W. Ertmer, Phys. Rev. Lett. **80**, 3173 (1998).
- [29] K. Sengstock, Ph.D. thesis, Universität Bonn, 1992.
- [30] G. Risberg, Ark. Fys. **28**, 381 (1964).
- [31] T. E. Mehlstäubler, Ph.D. thesis, Universität Hannover, 2005.
- [32] N. F. Ramsey, *Molecular Beams* (Clarendon Press, Oxford, 1956).
- [33] G. Jönsson, S. Kröll, A. Persson, and S. Svanberg, Phys. Rev. A **30**, 2429 (1984).
- [34] V. A. Dzuba, V. V. Flambaum, and M. G. Kozlov, Phys. Rev. A **54**, 3948 (1996).
- [35] V. A. Dzuba, M. G. Kozlov, S. G. Porsev, and V. V. Flambaum, Zh. Eksp. Teor. Fiz. **114**, 1636 (1998) [J. Exp. Theor. Phys. **87**, 885 (1998)].
- [36] C. Froese Fischer, G. Tachiev, and A. Irimia, At. Data Nucl. Data Tables **92**, 607 (2006).
- [37] S. G. Porsev, M. G. Kozlov, and Yu. G. Rakhlina, Pis'ma Zh. Eksp. Teor. Fiz. **72**, 862 (2000) [JETP Lett. **72**, 595 (2000)].
- [38] S. G. Porsev, M. G. Kozlov, Yu. G. Rakhlina, and A. Derevianko, Phys. Rev. A **64**, 012508 (2001).
- [39] J. Olsen, M. Godefroid, P. Jönsson, P. Malmquist, and C. Froese Fischer, Phys. Rev. E **52**, 4499 (1995).
- [40] A. Derevianko, W. R. Johnson, V. D. Ovsiannikov, V. G. Pal'chikov, D. R. Plante, and G. von Oppen, Phys. Rev. A **60**, 986 (1999).
- [41] C. Laughlin, E. R. Constantiniades, and G. A. Victor, J. Phys. B **11**, 2243 (1978).
- [42] J. E. Hansen, C. Laughlin, H. W. van der Hart, and G. Verbockhaven, J. Phys. B **32**, 2099 (1999).
- [43] T. Chanelière, J. L. Meunier, R. Kaiser, Ch. Miniatura, and D. Wilkowski, J. Opt. Soc. Am. B **22**, 1819 (2005).
- [44] J. Lawall, S. Kulin, B. Saubamea, N. Bigelow, M. Leduc, and C. Cohen-Tannoudji, Phys. Rev. Lett. **75**, 4194 (1995).
- [45] E. A. Curtis, C. W. Oates, and L. Hollberg, J. Opt. Soc. Am. B **20**, 977 (2003).
- [46] R. Santra, K. V. Christ, and Ch. H. Greene, Phys. Rev. A **69**, 042510 (2004).
- [47] A. Derevianko, Phys. Rev. Lett. **87**, 023002 (2001).